Apparatus for dynamical thermal measurements of low-thermal diffusivity particulate materials at subambient temperatures

Vladimir V. Murashov and Mary Anne White[a)]
Department of Chemistry, Dalhousie University, Halifax, Nova Scotia, B3H 4J3, Canada

(Received 30 June 1998; accepted for publication 15 September 1998)

Apparatus for measurement of thermal diffusivity of particulate matter in the temperature range of 10–300 K is described. The basis of the measurement is modulated radial heat flow into a cylindrical sample, with a relatively small temperature gradient. Data is analyzed by Fourier transformation, and thermal diffusivity is determined from both the phase lag and amplitude ratio of the temperature at various locations along the cross section of the cylinder. This apparatus was tested with solid benzene, and found to give measurements within $\pm 30\%$, in accord with the error analysis. It is especially useful for the determination of low thermal diffusivity materials, in the range of 1×10^{-8} to 5×10^{-6} $m^2\,s^{-1}$. © *1998 American Institute of Physics.* [S0034-6748(98)02112-1]

I. INTRODUCTION

Most solid dielectric materials exist in microcrystalline form, as particulate materials (loose powders) or microcrystalline conglomerates. Knowledge of the effective thermal conductivity and thermal diffusivity of particulate materials is required in the designs of thermal insulation, refractory materials, and cryogenic adsorbance vacuum systems; this information is also required for modeling studies of heat dissipation in the upper layers of the earth's crust (e.g., in the modeling of surface and underground explosions; in estimation of heat dissipation from buried power-line cables and hot water and steam lines), and at the surfaces of planets. Furthermore, it is desirable to be able to perform thermal measurements on particulate materials with as little alteration of the original sample as possible: for example, formation of a conglomerate from a powder involves the risk of alteration of the main phase due to either pressure-induced plastic and elastic deformations or pressure-induced solid-state phase transitions.[1]

Several techniques have been developed for measurement of thermal transport properties of dielectric particulate materials (usually very poor heat conductors),[2] and these can be divided into two groups: quasidynamical and dynamical, where the former deals with steady-state heat flow and the latter employs modulated heat flow. Further classification involves subdivisions, e.g., according to the apparatus geometry, method of heating, and temperature sensing.[3,4] In dynamical methods, the temperature field inside the sample is variable in time, and therefore these methods provide information about relaxation properties of the sample, i.e., thermal diffusivity, D. The thermal conductivity coefficient, κ, can be calculated from

$$\kappa = DC, \tag{1}$$

where C is the heat capacity per unit volume.

The superior performance of the dynamical methods (their high sensitivity, accuracy and temperature resolution, and applicability over a wide temperature range) determined the choice of the technique to be used here to design an apparatus for thermal measurements of low-diffusivity particulate materials. Among dynamical methods, those employing high-energy pulse heating (such as heating by irradiation with beams of high-energy elementary particles) are the most popular and productive for measuring thermal diffusivity of solids. However, these techniques do not permit measurement of extremely low diffusivity; for example, the lower bound of thermal diffusivity measured using lasers is estimated[5] to be 10^{-7} $m^2\,s^{-1}$, while some powders of practical importance have lower values (e.g., for water-loaded NaY zeolite,[6] $D=1.9\times10^{-8}$ $m^2\,s^{-1}$). Transient hot wire and differentiated line-heat source methods have been shown to be superior in sensitivity, accuracy, temperature resolution, and time consumption in measurements of loose particulate materials.[4] The former method was also shown to be well suited for high-pressure measurements of thermal properties of powders.[7,8] Measurements of loose evacuated powders are regularly accomplished with relatively high temperature gradients, ~20 K, although measurements with lower temperature gradients, ~5 K, have been reported.[9]

In this investigation, the modulated radial-heat flow technique in the converging geometry (i.e., with heaters located on the periphery of the cylindrical cell) was chosen. This configuration allows for easy sample change in a controlled atmosphere, and relatively small temperature gradients can be used. Automated data collection and analysis can be easily accomplished. Similar methods have been successfully applied to measure thermal diffusivity of a diversity of materials, such as ceramic specimens,[10,11] molten glass[12] and metals.[13] The major advances reported here are that Fourier analysis of the data allows sensitive determination of low thermal diffusivity with relatively small temperature gradients (less than 1 K), allowing meaningful determination of the temperature dependence of thermal diffusivity/thermal

a)Author to whom correspondence should be addressed; electronic mail: Mary.Anne.White@DAL.CA

conductivity, with the sensitivity optimized by a combination of temperature amplitude and temperature phase lag measurements. This method can allow determination of changes in thermal conductivity during, for example, phase transformations and lattice dynamics of particulate materials. Testing of the present apparatus was accomplished with measurements of solid benzene frozen into the cell.

II. THEORY OF MODULATED HEAT FLOW IN A CYLINDRICAL CELL

The design of the experimental cell was chosen to satisfy the approximation of an infinite cylinder to avoid theoretical complications associated with heat dissipation at the cylinder ends. To meet this approximation, the height of the cylinder, H_{cell}, has to be at least three times the diameter of the cylinder, $2R_{\text{cell}}$. Using this approximation, the time dependence of the temperature at the point located at a distance r from the axis of the cylinder is given by[14]

$$\frac{\partial T}{\partial t} = D\left(\frac{\partial^2 T}{\partial r^2} + \frac{1}{r}\frac{\partial T}{\partial r}\right). \tag{2}$$

Assuming that the initial temperature across the cylinder is uniform and equal to T_0 (i.e., at $t=0$ for all r, $T=T_0$) and at time $t>0$ a sinusoidally modulated Joule energy input, of frequency ω, is applied to the cylindrical surface at distance r_0 from the axis of the cylinder, causing a corresponding change of the surface temperature, then

$$T - T_0 = T_A(r=r_0)\cos(\omega t), \tag{3}$$

where T_A is the amplitude of the temperature wave, and the following solution can be obtained:[12]

$$\frac{T-T_0}{T_A(r=r_0)} = \frac{\cos(\omega t)ber(z) + \sin(\omega t)bei(z)}{ber^2(z)+bei^2(z)}, \tag{4}$$

where $z=r_0(\omega/D)^{1/2}$ and $ber(z)$ and $bei(z)$ represent the Thompson (also known as Bessel real and imaginary) functions, defined through the modified Bessel function of the zeroth order, I_0, as:[15]

$$ber(z) + i\cdot bei(z) = I_0(zi^{1/2});$$
$$ber(z) - i\cdot bei(z) = I_0(zi^{-1/2}). \tag{5}$$

The solution of Eq. (4) for maxima by zeroing the time derivative gives the following formula for the phase lag, $\Delta\Theta$, between temperature waves at the perimeter $r=r_0$ (and at the center of the cylindrical sample $r=0$), (see Fig. 1):

$$\tan\Delta\Theta = \frac{bei(z)}{ber(z)}. \tag{6}$$

Thus, knowing z, thermal diffusivity can be calculated from the following expression:

$$D = \omega r^2/z^2. \tag{7}$$

The decay of the temperature wave is also related to the thermal diffusivity and, therefore, it can be used for diffusivity determinations. For example, it has been shown that diffusivity can be calculated from the correlation between the amplitudes of thermal waves on the surface of the cylindrical sample obtained for two different frequencies.[13] Therefore,

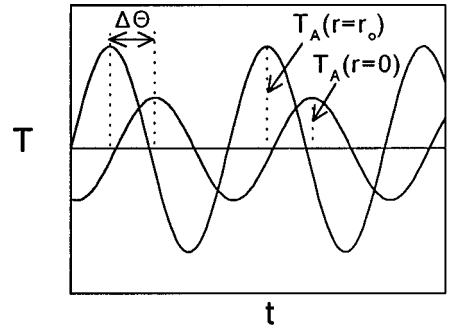

FIG. 1. Schematic of a temperature wave inside a cylindrical sample that is heated with sinusoidally modulated power at the center ($r=0$) and at some distance (r_0) from the axis as a function of time, showing the phase lag, $\Delta\Theta$.

Eq. (6) can be used further to express z through the ratio of amplitudes of the temperature wave at the perimeter $[T_A(r=r_0)]$ and at the center of the cylindrical sample $[T_A(r=0)]$ (see Fig. 1), as follows:

First, sine and cosine can be expressed through the Thompson functions as

$$\sin\Delta\Theta = \frac{bei(z)}{[ber^2(z)+bei^2(z)]^{1/2}} \tag{8}$$

and

$$\cos\Delta\Theta = \frac{ber(z)}{[ber^2(z)+bei^2(z)]^{1/2}}. \tag{9}$$

Next, this pair of expressions can be substituted into Eq. (4) to obtain an expression for the ratio of the temperature amplitudes (considering only positive values of the amplitude ratio to be physically meaningful)

$$\frac{T_A(r=0)}{T_A(r=r_0)} = \frac{1}{[ber^2(z)+bei^2(z)]^{1/2}} = \frac{1}{M_0(z)}, \tag{10}$$

where $M_0(z)$ is the modulus of the modified Bessel function of the first kind of zeroth order.

Equation (10) relates the temperature amplitude ratio to z; this will be used for thermal diffusivity calculations in the ''amplitude'' method, as distinguished from the ''phase'' method, which employs Eq. (6) and the phase lag.

Figure 2(a) illustrates the dependence of the phase lag and amplitude decay on the parameter z. At small values of z, the modulus of the modified Bessel function grows more gradually compared with the phase of the function, and therefore at small values of z a larger uncertainty in z can be expected for a given uncertainty in $M_0(z)$ compared with the same uncertainty in $\Delta\Theta$. To investigate error propagation during evaluation of z from either the phase lag or amplitude attenuation, it is illustrative to calculate a propagation coefficient, A_{prop}, connecting the error in variable, x, and the error in function, y, as: $(dy/y)=A_{\text{prop}}(dx/x)$. It follows from the definition that $A_{\text{prop}}=x(d\ln y/dx)$. Figure 2(b) shows that the threshold value of z, at which the ''amplitude'' and ''phase'' methods swap their performance during Bessel function evaluation, lies at around 2.7. The amplitude method can be expected to perform better at values for $z>2.7$. In the phase method the uncertainty is nearly constant for transformation of the phase lag into z for z ranging from

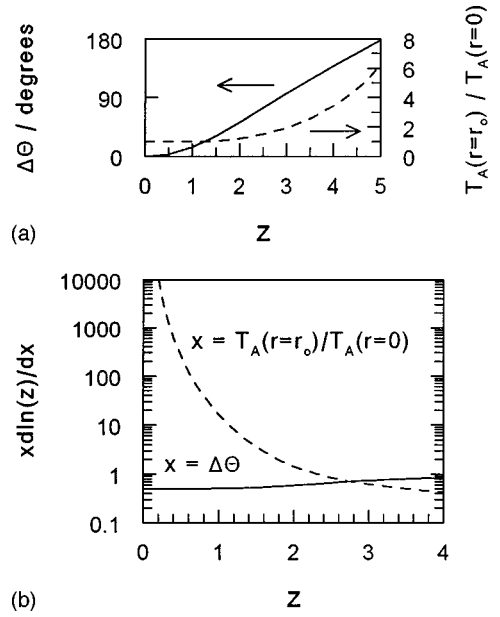

FIG. 2. (a) Dependence of the phase lag (solid line) and the ratio of the amplitudes of thermal waves at the center and at a distance r_0 from the center (dashed line) on the Bessel function parameter z. (b) Dependence of the error propagation factor in the phase method (solid line) and in the amplitude method (dashed line) on z.

0 to 4, whereas the amplitude method results in a significant magnification of the error for $z<2$. It is possible to use the differences between results obtained with the phase and amplitude methods to evaluate systematic errors.[1]

III. SAMPLE ASSEMBLY

The thermal conductivity/diffusivity calorimeter is shown schematically in Fig. 3. The sample was contained in the inner cell cylinder, with height $H_{\text{cell}}=0.06$ m and inner diameter $2R_{\text{cell}}=0.018$ m; this fit snugly in the outer cell cylinder. Both cylinders were made of brass. The space between the two cylinders was filled with Apiezon *N* vacuum grease[16] for good thermal contact. The sample heater was made of double-silk covered 38 SWG manganin wire (25 $\Omega\ \text{m}^{-1}$ resistance) wound bifilarly around the outer cell cylinder and varnished into place with low-temperature GE 7031 varnish (TRI Research, Inc.). There were five 0.08-mm-diam Au-0.03% Fe/Chromel differential thermocouples (Johnson Matthey; supplied and calibrated by Cryogenic Calibrations Ltd., England, with accuracy ± 0.05 K from 30 to 300 K), each held in a ceramic tube of 1.8 mm o.d. and 0.9 mm i.d. (Omega Engineering, Inc.). The tubes were aligned along the axis of the cell, allowing measurement of the temperature variation at the axis of the cell and at four equally spaced positions on a circle with radius 5 mm (see Fig. 3). The tubes were sealed into a phenolic disk with 1 h epoxy to which 5 mass % phenolic powder was added as a filler to reduce the coefficient of thermal expansion.[17] The same epoxy composite was used to make a vacuum-tight seal between a brass ring and the phenolic disk. The vacuum inside the inner cell cylinder was ensured by indium o-ring seals between the inner cell cylinder and the lid of the cell at the top of the assembly, and the brass ring of the phenolic disk at the bottom of the assembly.

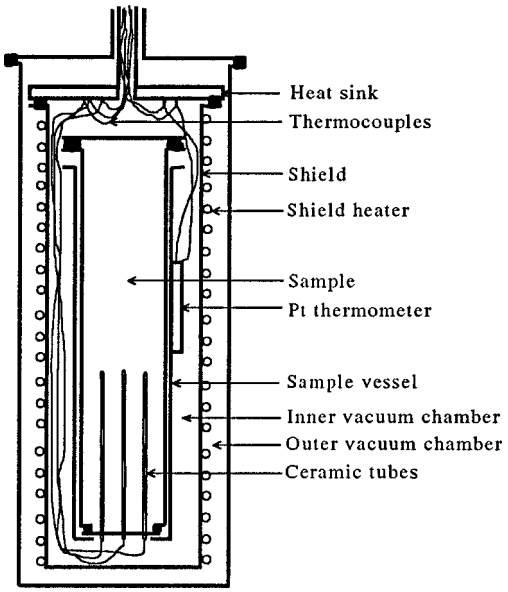

FIG. 3. Schematic diagram of the thermal conductivity apparatus measurement assembly.

A platinum resistance thermometer (Cryocal, PR-100, 20 Ω at $T=77$ K, calibrated by TRI Research) was inserted into a brass sleeve soldered to the outer cylinder. The space between the thermometer housing and the thermometer was filled with Apiezon *N* vacuum grease.

The variation of the temperature inside the sample relative to the heat sink was detected using the Au-0.03% Fe (one piece, 200 mm long)/Chromel (two pieces, 200 mm long each) differential thermocouples. Such long wires were used to minimize the flux of heat along them. The junctions were made by spark welding in a helium atmosphere.[18]

For better control of heat dissipation by the cell and to accommodate adiabatic requirements of adiabatic calorimetry (for determination of heat capacity using the same apparatus) the cell was suspended on nylon line inside another brass cylinder (further referred to as the shield, see Fig. 3). A three-section heater made of double-silk wound 38 SWG manganin wire (25 $\Omega\ \text{m}^{-1}$ resistance) was wound bifilarly around the shield and varnished into place with low-temperature GE 7031 varnish. Three pairs of differential thermocouples (Cu/Constantan)[19] were used in the circuits of the temperature controller: two were to minimize the temperature gradient along the shield and one was to sustain the necessary temperature difference between the shield and the sample cell. There was an indium o-ring seal between the shield and the heat sink (see Fig. 3) and the space within the shield could be evacuated or filled with helium gas to allow better control of heat dissipation by the cell. To avoid contamination of the signal on the hot junctions of the thermocouples by modulations in the heat sink temperature, all measurements in the modulated energy flow regime were undertaken after evacuating the inner vacuum chamber of the apparatus with a roughing pump.

During operation, the cell assembly is immersed in an appropriate cryogen (liquid nitrogen for $T>80$ K, liquid helium for $10\ \text{K}<T<80$ K).

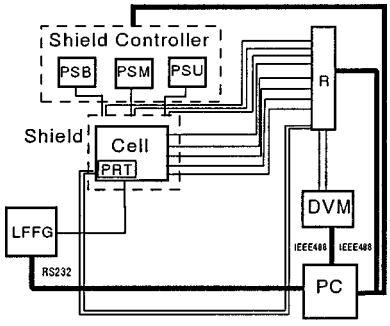

FIG. 4. Block diagram of the thermal conductivity apparatus. PC: personal computer; RS232: serial interface; IEEE488: parallel interface; LFFG: programmable low-frequency function generator; DVM: digital voltmeter; PRT: platinum resistance thermometer; PSU: power supply for the upper heater; PSM: power supply for the middle heater; PSB: power supply for the bottom heater; R: relay control. Thin connecting lines denote double wires.

IV. ELECTRONICS AND MEASUREMENT PROCEDURE

The experimental apparatus was built to require minimum participation of the operator, and therefore all the electronics and most operations are controlled by computer. The general plan of the electronics is given in Fig. 4. The computer employed is an IBM-PC compatible computer with a 80486DX2-S microprocessor with mathematical coprocessor, 66 MHz clock, 640 kbytes of base memory, 3072 kbytes of extended memory, and 256 kbytes of cache memory. A multifunctional Hewlett–Packard 3456A digital voltmeter (DVM) is linked to the computer via the parallel IEEE488 interface.

A programmable ultralow frequency function generator (LFFG) was specially designed and built to meet the requirements of supplying a power signal with the required time profile, i.e., tunable frequency in the range between 0.001 and 3 Hz, with variable power of up to 5 W. The power supply is characterized by 12 bit (i.e., 1 part per 4096) function resolution and scaling resolution and requires 256 floating point entries between 0.0 and 1.0 for unipolar output and from -1.0 to $+1.0$ for bipolar output to define one period of a normalized wave. In the modulated energy flow regime a table of 256 floating-point values of $[0.5\sin(x_i)+0.5]^{1/2}$ representing one period of a normalized sine wave of power, where $x_i=2\pi i/256$ for i from 0 to 255, are sent to the LFFG. To get a dc pulse in the constant energy flow regime (required during temperature stabilization) a table of 256 units was used. Communication with the computer was realized through the serial RS-232 interface.

A triple programmable power supply was built to provide the required power to the three shield sections (upper, middle, and lower): a maximum power of 5 W (with 12 bits resolution in voltage) could be applied to each section.

A relay control containing 11 mechanical switches was used to select a sensor whose signal is to be directed to the DVM for acquisition. The DVM takes readings of the electromotive force (emf) created between the cold and hot ends of the differential thermocouples, or resistance of the platinum thermometer in the four-wire Ω mode with terminal emf compensation.

The parallel IEEE488 interface was used to control both the shield power supply and the relay.

Control over the experiment was realized in the QuickBasic environment. As the speed of the program execution is not a limiting factor in these measurements, the codes were run under the QuickBasic interpreter. At the beginning, the program initializes interfaces, checks and resets administered electronics, and identifies operational thermocouples. After that the computer stabilizes the temperature of the cell at the required value, or identifies the lowest achievable temperature in that particular heat exchange regime, by manipulating the power applied to the three-section shield heater using the proportional-integral-differential (PID) controller algorithm with predetermined parameters for operational heat exchange regimes.

In the modulated energy flow regime, an equivalent dc power is applied to the cell during temperature stabilization to simulate an offset power of the modulated energy pulse and therefore prevent an increase of the sample temperature during measurements. When the temperature drift rate is brought to a magnitude less than the threshold value (corresponding to a change of mean sample temperature less than 1 K during data acquisition for one temperature point, i.e., drift rate less than about 3×10^{-5} K s^{-1}), a sine wave of power of the desired frequency and amplitude generated by the LFFG is applied during the period required to collect a preset number of points and cycles. The power applied to the three-section heater of the shield is kept constant to prevent contamination of the time dependence of the temperature field in the sample by low-frequency fluctuations due to stabilization of the average temperature of the calorimeter. Upon completion of the data collection at one temperature, the program automatically heats the cell to the next temperature point using the preset value of the temperature step, which is typically 10 K. Then the temperature is stabilized and measurements are taken again.

V. DATA ACQUISITION AND ANALYSIS

Data from a run contain records of the time of collection, the temperature at the surface of the cell as detected by the platinum resistance thermometer, and values of emfs at the sample- (heat sink) and cell-shield differential thermocouples. The number of points accumulated during the modulated energy-flow regime has to be a power of 2 to allow for the fast Fourier transformation (FFT), and, hence, during a regular run 1024 data points ($2^{N'}$ with $N'=10$) were collected with 10 points per cycle.

The discrete Fourier transform maps the $2^{N'}$ experimental values of a time-dependent variable, such as temperature (or emfs), T_k, onto $2^{N'}$ complex numbers $F_T(f_n)$ according to the formula:

$$F_T(f_n)=2^{1-N'}\sum_{k=0}^{2^{N'}-1} T_k e^{2^{1-N'}\pi ikn}. \tag{11}$$

Thus, the Fourier transformation yields information about the temperature waves at the cell surface and inside the sample in the form of spectra in complex space, and the

magnitudes of the real and imaginary parts, and therefore, the amplitudes and phases of the waves can be obtained. Fourier transformation of the experimental data points is performed using a fast Fourier transform algorithm, implemented in a standard Basic routine.[20]

The shifting theorem[21] allows investigation of the phase difference between the signals of interest. If, for a given frequency f_s, Fourier transforms of signals 1 and 2 are given by

$$F_{T1}(f_s)=a_1+b_1 i; \quad F_{T2}(f_s)=a_2+b_2 i, \tag{12}$$

respectively, then signal phases, Θ, with respect to the beginning of the sampling for each signal, t_1 and t_2, are

$$\Theta_1=\arctan(b_1/a_1); \quad \Theta_2=\arctan(b_2/a_2), \tag{13}$$

and the amplitudes of the waves, T_A, are found as

$$T_{A1}=(a_1^2+b_1^2)^{1/2}; \quad T_{A2}=(a_2^2+b_2^2)^{1/2}. \tag{14}$$

Thus the phase difference between the two signals, $\Delta\Theta$, is

$$\Delta\Theta=\Theta_2-\Theta_1+(t_2-t_1)2\pi f_s. \tag{15}$$

In the next stage of our thermal diffusivity data analysis, specially written routines calculate the parameter, z, of the modified Bessel function of the first kind of zeroth order for a given phase and amplitude ratio. This is accomplished by means of series summation until the convergence criterion for the Bessel function series is less than 10^{-3}%. (As these series are alternating, the infinite sum over the remaining terms is less than the absolute value of the cutoff term.)

The temperature of the surface of the cell is recovered from resistance values using a spline function fitted to the Pt thermometer calibration data.

VI. ERROR ANALYSIS

The main sources of errors include: measurements, data analysis, and assumptions used in the theoretical models. The largest experimental errors are temperature uncertainty, giving rise to random error, and uncertainty in the positions of thermocouples, which leads to systematic error.

Thermal fluctuations in emf in thermocouples (<10 μV)[22] and thermal fluctuations in the platinum resistance thermometer (PRT) lead to random errors and these can be reduced by averaging in either the Fourier transform routine (emf) or linear least-square fit (PRT). Analysis of the spectra of emf indicates that statistical error in the measured emf due to the noise in the electronics and thermal fluctuations in temperature sensors left after averaging over 2^{10} points ($\sim$100 cycles) can be maintained under 5% (except for the lowest temperatures when a low power signal is required and this error can increase to 20%) for the amplitude of the temperature wave and around $2^{1/2}$ times that for the real and imaginary parts of the wave. Calibration accuracy of the PRT temperature is $\pm$0.01 K and therefore uncertainty at 100 K is 0.01%. Uncertainty in the PRT temperature due to self heating in the four-wire method with compensation for thermal emf can be neglected. Temperature drift allowed during diffusivity measurements was 1 K per period of data accumulation, and therefore uncertainty in the temperature in the modulated-energy-flow technique can be accepted as 0.5 K.

Uncertainty in the positions of thermocouple junctions gives rise to systematic error that can be estimated as $\sim$5%. Averaging over all four thermocouples reduces this uncertainty.

Uncertainty in frequency gives statistical error that can be estimated as half the frequency resolution, i.e., $df/2$, normalized with the working frequency, which leads to error in frequency given by the reciprocal of the number of cycles collected. Thus, it is 1% for 100 cycles collected.

Random errors acquired during data analysis are small (e.g., uncertainty in the determination of the Bessel function parameter z is less than 0.001%) and can be neglected in the thermal diffusivity measurements.

The theoretical model assumptions used in the data analysis could give rise to systematic errors. The data analysis is based on the following suppositions: the material is homogeneous; the cell is an infinite cylinder (in diffusivity and thermal conductivity measurements); the thermal sensors do not affect the temperature distribution in the sample; the thermal properties of the sample do not change with time; there is an ideal thermal contact between the thermal sensors and the sample. The effect of heat dissipation by the finite sample boundaries was shown to be negligible for a threefold ratio of length to diameter used in this work.[23] Other types of errors are difficult to estimate.

Assuming errors described above, the overall relative error of diffusivity measurements, $\delta D/D$, arising from errors in frequency, $\delta f/f$, in the position of thermocouple junctions in the sample, $\delta r/r$, and in the z parameter, $\delta z/z$, can be estimated as[24]

$$\delta D/D=|\delta f/f|+2|\delta r/r|+2|\delta z/z|, \tag{16}$$

where $\delta z/z \approx |\delta\Delta\Theta/\Delta\Theta|$ for the phase method. The error in the phase lag, $\delta\Delta\Theta/\Delta\Theta$, is estimated as 11% for 30° phase lag, assuming 7% error in the complex components of emf. Thus, overall uncertainty of the phase method in the diffusivity measurements [Eq. (16)] can be estimated as $1\%+2\times5\%+2\times11\%=33\%$. In the case of the amplitude method, uncertainty in the ratios of wave amplitudes gives $\delta z/z$ of 10% and thus overall uncertainty in thermal diffusivity can be taken as 31% for the amplitude method.

Discrepancies in the results of phase and amplitude methods of data analysis of experimental measurements of thermal diffusivity can be used to estimate error in the measurements and extract a ''real'' thermal diffusivity, with an uncertainty of $\sim$30%.[1]

VII. TEST MEASUREMENTS

The apparatus was tested with solid bulk material to avoid complications of powders. Solid benzene (ACS grade, 99% pure, purchased from AnalR and dried for 6 h over molecular sieves), frozen into the cell, was found to be satisfactory for testing.

Experimental thermal diffusivity data estimated with both phase and amplitude methods [Eqs. (6), (7), and (10)]

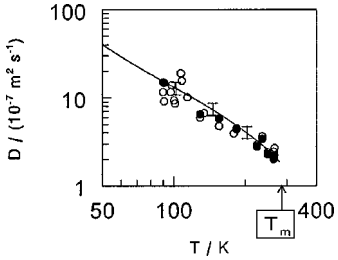

FIG. 5. Experimental values of thermal diffusivity of solid benzene. Open circles denote points obtained with the phase method; filled circles denote points obtained with the amplitude method. A fit to literature values (Refs. 25–27) is represented by the solid line (bars show ±10% range). T_m represents the melting point of benzene.

are shown in Fig. 5 along with literature values obtained by fitting experimental data for benzene's thermal conductivity,[25] heat capacity,[26] and volume thermal expansion.[27] There is a good agreement between results obtained with the modulated-radial-energy flow apparatus and data reported elsewhere. Scatter of the experimental points is within 25% at temperatures between 110 and 300 K, which is in agreement with the estimate of the experimental uncertainty given above. At temperatures between 85 and 110 K, scatter can be as high as 50%; this could be related to loosening of the thermal contact between the junctions of thermocouples and solid benzene due to differences in coefficients of thermal expansion. The phase and the amplitude methods were found to perform with similar accuracy and precision for values of z around 3.

This apparatus was also used to measure thermal diffusivity of particulate materials in the temperature range between 10 and 80 K using liquid helium as a coolant.[1]

VIII. DISCUSSION

The present apparatus is found to be capable of measuring thermal diffusivity in the range between 1×10^{-8} and 5×10^{-6} $m^2\,s^{-1}$, but extension of this range is possible.

The lower bound of the measured thermal diffusivity is restricted by heat leaks along the thermocouple wires, by the upper limit of power applied to the surface (leading to higher temperature gradients), and by the sensitivity of temperature sensors. Heat leaks can be reduced by better thermal insulation of the base of the cell and/or further increase in the length-to-width ratio of the cell.

The higher diffusivity bound results from the upper bound of the working frequency, which in turn is determined by the time required to perform all measurements with one voltmeter. Allocation of a separate measuring device to monitor the most time consuming procedure, viz., PRT resistance measurements, could be used to increase the upper bound on thermal diffusivity.

Sensitivity of the apparatus is limited by the resolution of the DVM engaged with the apparatus and the sensitivity of the temperature detectors. Resolution of the DVM used in this work (HP3456A) is 0.1 μV, therefore the lower bound of uncertainty is 0.05 μV. A signal with about 20% uncertainty corresponding to a temperature wave amplitude of 0.02 K in the center of the cell can be created by an order of magnitude larger temperature wave on the surface of the cell (for a sample with thermal diffusivity of around 10^{-7} m^2 s). Thus, the temperature gradient used can be under 1 K for low-thermal diffusivity materials which is significantly lower than the usual temperature gradients employed in the measurements of thermal conductivity/diffusivity of evacuated loose dielectric powders.

In order to reduce statistical error, averaging over a large number of cycles can be used. On the other hand, long runs make it difficult to maintain stable mean temperatures. For this reason, the dependence of the scatter of the thermal diffusivity values on the number of data points was investigated. It was found that the minimum number of points to reduce statistical noise below the DVMs sensitivity level, while maintaining a small temperature gradient, is 2^{10} (corresponding to ~100 cycles).

This apparatus can be also used for heat capacity measurements (as an adiabatic calorimeter) and thermal conductivity measurements (in the modulated-heat flow regime after estimation of the energy flux applied to the sample) requiring only some changes in the control software apparatus and heat exchange conditions.[1] As for Fourier spectroscopies, application of the Fourier transform data analysis allows significant improvements in sensitivity of the apparatus.

ACKNOWLEDGMENTS

The authors thank B. Millier and C. Wright for building the electronics for the apparatus, and R. Conrad, B. Eisener, and R. Shortt for machining the calorimeter. We also thank the Natural Sciences and Engineering Research Council of Canada for financial support through Research and Equipment Grants to MAW. This work was also supported by the Killam Trusts (Scholarship to VVM and Research Professorship to MAW).

[1] V. V. Murashov, Ph.D. thesis, Dalhousie University, Halifax, NS, Canada, 1998.
[2] W. Woodside and J. H. Messmer, J. Appl. Phys. **32**, 1688 (1961).
[3] *Compendium of Thermophysical Property Measurement Methods*, edited by A. Cezairliyan and V. E. Peletsky (Plenum, New York, 1992).
[4] For the most recent review of methods used for measurements of thermal conductivity of particulate materials see: M. A. Presley and P. R. Christensen, J. Geophys. Res. **102**, 6535 (1997).
[5] K. D. Maglic and R. E. Taylor in: *Compendium of Thermophysical Property Measurement Methods*, edited by A. Cezairliyan and V. E. Peletsky (Plenum, New York, 1992), Vol. 2, p. 281.
[6] J. Völkl in: *Proceedings of the 7th International Heat Transfer Conference*, Munich, 1982 (Hemisphere, Washington, 1982), Vol. 2, p. 105.
[7] G. Bäckström in: *Proceedings of the 7th Symposium Thermophys. Prop.*, edited by A. Cezairliyan (ASME, New York, 1977), p. 169.
[8] B. Håkansson, P. Andersson, and G. Bäckström, Rev. Sci. Instrum. **59**, 2269 (1988).
[9] R. B. Merrill, NASA TN D-5063, Washington, 1969 (unpublished).
[10] H. Rouault, J. Khedari, C. Arzoumanian, and J. Rogez, High Temp.-High Press. **19**, 357 (1987).
[11] H. Fujisawa, N. Fujii, H. Mizutani, H. Kanamori, and S. Akimoto, J. Geophys. Res. **73**, 4727 (1968).
[12] A. F. van Zee and C. L. Babcock, J. Am. Ceram. Soc. **34**, 244 (1951).
[13] L. P. Filippov and L. A. Pigal'skaya, Teplofiz. Vys. Temp. **2**, 384 (1964).
[14] H. S. Carslaw and J. C. Jaeger, *Conduction of Heat in Solids*, 2nd ed. (Clarendon, Oxford, 1986).
[15] N. W. McLachlan, *Bessel Functions for Engineers*, 2nd ed. (Clarendon, Oxford, 1961).

[16] A. J. Gordon and R. A. Ford, *The Chemist's Companion: A Handbook of Practical Data, Techniques, and References* (Wiley, New York, 1972).
[17] Thermal expansion of brass: J. J. M. Beenakker and C. A. Swenson, Rev. Sci. Instrum. **26**, 1204 (1955); thermal expansion of epoxies: W. O. Hamilton, D. B. Greene, and D. E. Davidson, Rev. Sci. Instrum. **39**, 645 (1968); thermal expansion of ceramics: G. K. White, Crystallogr. Rep. **16**, 487 (1976); thermal expansion of phenolic-fiber composites: J. T. Mottram, B. Geary, and R. Taylor, J. Mater. Sci. **27**, 5015 (1992).
[18] R. L. Rosenbaum, Rev. Sci. Instrum. **39**, 890 (1968).
[19] L. L. Sparks and R. L. Powell, Crystallogr. Rep. **12**, 40 (1972).
[20] H. W. Press, B. P. Flannery, S. A. Teukolsky, and W. T. Vetterling, *Numerical Recipes* (Cambridge University Press, Cambridge, 1990).
[21] H. J. Weaver, *Theory of Discrete and Continuous Fourier Analysis* (Wiley, New York, 1989).
[22] G. K. White, *Experimental Techniques in Low-Temperature Physics*, 3rd ed. (Oxford University Press, Oxford, 1979).
[23] Ya. A. Kirichenko, Teplo i Massoper., Pervoe Vses. Soveshch., Minsk (1961) **1**, 77 (1962).
[24] L. G. Parrat, *Probability and Experimental Errors in Science; An Elementary Survey* (Dover, New York, 1971).
[25] R. G. Ross, P. Andersson, and G. Bäckström, Mol. Phys. **38**, 527 (1979).
[26] G. D. Oliver, M. Eaton, and H. M. Huffman, J. Am. Chem. Soc. **70**, 1502 (1948).
[27] E. R. Andrew and R. G. Eades, Proc. R. Soc. London, Ser. A **218**, 537 (1953).